Dyes and Pigments 172 (2020) 107801

Contents lists available at ScienceDirect

Dyes and Pigments

journal homepage: www.elsevier.com/locate/dyepig

Water-soluble 4-hydroxystyryl and 4-hydroxyphenyl-butadienyls dyes with switchable fluorescence

Kateryna Bondar, Maksym Bokan, Gary Gellerman, Leonid D. Patsenker*

Department of Chemical Sciences, Ariel University, Ariel, 40700, Israel

ARTICLE INFO

Keywords:
4-Hydroxystyryl
4-Hydroxyphenyl-1,3-butadienyl
Switchable fluorescence
Fluorescence ratiometry
Protolytic properties
Drug delivery monitoring

ABSTRACT

Fluorescent 4-hydroxystyryl dyes are useful for many biomedical and pharmaceutical assays, and other analyte sensing applications. However, these dyes often suffer from limited applicability in analytical and bioanalytical utilization due to insufficient water-solubility, high acid-ionization constants (pK_a) and short-wavelength absorption and emission. To solve these issues, a series of new, water-soluble 4-hydroxystyryl and longer-wavelength 4-hydroxyphenyl-butadienyl dyes were synthesized and the spectral and protolytic properties were studied. These new dyes contain electron-withdrawing substituents *ortho* to the triggering 4-hydroxyl group. The introduction of the cyano and formyl groups was found to decrease the pK_a and extend the pH-sensing region of these fluorophores. In respect of the molecular structure, these dyes exhibit either a "turn-on" activatable fluorescence, or a dual-fluorescence that enables ratiometric measurements. The 4-hydroxyphenyl-butadienyl dye was evaluated for fluorescence monitoring of drug delivery. These new dyes are promising fluorophores for acidity measurements and other sensing applications.

1. Introduction

Fluorescent dyes sensitive to acidity [1], intracellular pH [2], presence of ions [3], drugs [4], enzymes [5], small molecules [6], and high-molecular-weight analytes [7] are widely used in medical diagnosis and fluorescence-guided surgery [8], targeted drug delivery monitoring [9], imaging [10], biomedical and pharmaceutical research [11], environment monitoring [12], control of chemical processes [13], and other sensing applications [14]. Many sensing dye molecules comprise 4-hydroxystyryl fluorophore conjugated with a heterocyclic terminal end-group in particular a quaternized indolenine moiety [15]. These 4-hydroxystyryl dyes were proposed for detection of fluoride (F^-) [16], sulfite (SO_3^{2-}), bisulfite (HSO_3^-), bisulfate (HSO_4^-) [17], sulfur dioxide (SO_2) [18], hydrogen sulfide [19], thiophenols [20], hydrazine [21], mercury (Hg^{2+}) [22], and cysteine (Cys) in living cells [23].

The operative principle of these 4-hydroxystyryl dyes consists in cleavage (sometimes addition) of an analyte-sensitive trigger group attached to the 4-hydroxyl functionality, which results in a pronounced change in the spectral properties due to the formation of negatively charged phenolate anion [16,23] (Scheme 1). When the trigger substituent is a proton, the reversible protonation-deprotonation can designate the dye as a pH sensor. Analyte-mediated cleavage of the trigger group causes a decrease of the absorption band related to the non-fluorescent "Off" form and an increase of the new, longer-wavelength absorption and emission bands originated from the "On" form. In the more acidic media, when the oxygen atom is protonated, the spectral properties of 4-hydroxyl derivatives are similar to those for the *O*-substituted "Off" forms [24,25]. Such an effect was found in the series of many other dyes containing a conjugated hydroxylic group [26], e.g. fluoresceins [4,27], coumarins [28], imidazolinones [29], and 1-hydroxyperylene bisimides [30].

The ability of a 4-hydroxyl group for protonation-deprotonation leads to two main findings. First, the 4-hydroxystyryl dyes are able to perform as analyte-sensitive probes (sensitive to the trigger group cleavage) only within a certain pH range, which is above their pK_a. Second, due to the reversible protonation-deprotonation, these dyes can act as pH indicators.

Obviously, the pH range required for both the analyte sensing and pH probing applications can be extended by decreasing the dye pK_a, which can supposedly be achieved by introducing the electron-withdrawing substituents conjugated with the 4-hydroxyl group. Nevertheless, to the best of our knowledge, 4-hydroxystyryl dyes containing electron-withdrawing groups have not been previously synthesized and investigated as pH indicators or analyte-sensitive probes.

Importantly, many sensing applications in particular biomedical

* Corresponding author.
E-mail addresses: kateryna.bondar@msmail.ariel.ac.il (K. Bondar), maksymbo@ariel.ac.il (M. Bokan), garyg@ariel.ac.il (G. Gellerman), leonidpa@ariel.ac.il (L.D. Patsenker).

https://doi.org/10.1016/j.dyepig.2019.107801
Received 18 July 2019; Received in revised form 12 August 2019; Accepted 13 August 2019
Available online 14 August 2019

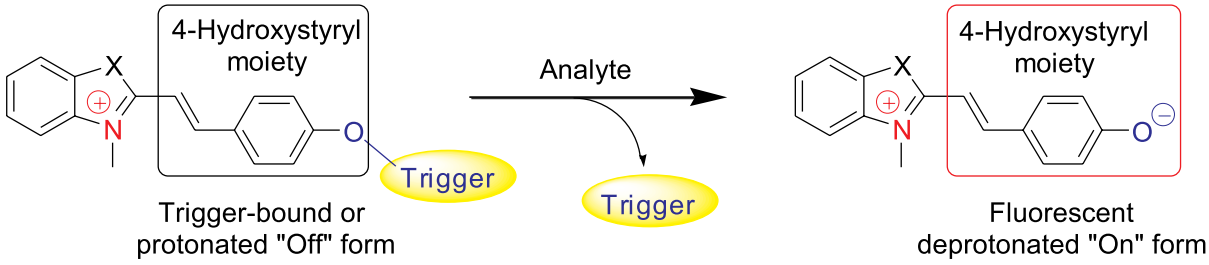

Scheme 1. Operative principle of analyte sensitive 4-hydroxystyryl dyes.

and pharmaceutical assays require water-soluble dyes or the dyes with an adjusted hydrophilic-hydrophobic balance [31]. The improved water-solubility helps to increase the dye concentration, reduce aggregativity in aqueous solutions, increase the signal-to-noise ratio, and avoid the non-specific interaction with high-molecular-weight analytes in biological systems.

Finally, the dyes emitting within the most transparent red and near-IR spectral range are beneficial for biomedical sensing applications, fluorescence imaging, diagnostics, and drug delivery monitoring [32]. Presumably, the absorption and emission bands of 4-hydroxystyryls can be red-shifted by introducing an additional double bond in the π-conjugated system to form 4-hydroxyphenyl-butadienyl dyes. However, none of these structures have previously been reported.

In this work, we synthesize and investigate a series of novel, water-soluble of 2-(4-hydroxystyryl)- (n = 1) and 4-hydroxyphenyl-butadienyl (n = 2) indolenine dyes containing electron-withdrawing cyano, formyl and carboxyl groups *ortho* to the 4-hydroxyl function (Scheme 2). Dye **St1** has previously been reported [18] while **St2–St6** are first synthesized and characterized in this research; the spectral and protolytic properties are studied. In addition, dye **St6** is tested as switchable reporter for drug delivery monitoring.

2. Materials and methods

2.1. General information

All chemicals were supplied by Alfa Aesar Israel. Solvents were purchased from Bio-Lab Israel and used as is. Cell culture medium (CM) was from Sigma-Aldrich. CM (500 mL) contained a RPMI-1640 standard cell culture medium (435 mL), esterases containing fetal bovine serum (50 mL), penicillin (10,000 U/mL, 5 mL), streptomycin (10 mg/mL, 5 mL), glutamine (200 mM, 5 mL), and phenol red indicator (5.3 mg/L). TLC plates (Silica gel 60 F-254) were from Merck.

^{1}H NMR and ^{13}C-NMR spectra were measured on a Bruker (400 MHz) spectrometer in DMSO-d_6. TMS was used as an internal standard.

High-resolution mass spectra (HRMS) were measured using an Agilent QTOF mass-spectrometer in electrospray ionization (ESI) positive ion mode.

LC/MS analyses were performed using an Agilent Technologies 1260 Infinity (LC) 6120 quadruple (MS), column Agilent SB-C18, 1.8 mm, 2.1 × 50 mm, column temperature 50 °C, eluent water — acetonitrile (CH_3CN) + 0.1% formic acid.

HPLC purifications were carried out on an ECOM preparative system, with dual UV detection at 230 nm and 254 nm. A Phenomenex Gemini® 10 mm RP18 110 Å, LC 250 × 21.2 mm column was used. The column was kept at 25 °C. Eluent A (0.1% TFA in water) and B (0.1% TFA in CH_3CN) were used. A typical elution was a gradient from 100% A to 100% B over 35 min at a flow rate of 25 mL/min.

Chemical reactions were monitored by TLC (Silica gel 60 F-254, Merck) and by LC/MS. The purities of the dyes were determined by LC/MS.

Absorption and fluorescence spectra were measured at 25 °C in 1 cm quartz cells at ~1 μM dye concentrations in 0.1 M buffer solutions of different pH. Absorption spectra were recorded on a Jasco V-730 UV–Vis spectrophotometer and the fluorescence spectra were measured on an Edinburgh Instruments FS5 spectrofluorometer. The recorded fluorescence spectra were corrected using the wavelength-dependent instrument sensitivity coefficients. Absorption and emission maxima were determined with accuracy of ± 0.3 nm and ± 0.5 nm, respectively, and rounded. The absorbances (A) of the samples and the reference at the excitation wavelength (λ_{Ex}) for the protonated dyes were in general 0.04–0.08 measured in a 1-cm cell. λ_{Ex} for the protonated forms was 405 nm for **St1**–**St4** and 430 nm for **St5**. λ_{Ex} for the deprotonated forms was 500 nm for **St1**, **St2**, **St4**, **St6**, 470 nm for **St3** and 560 nm for **St5**.

Molar absorptivity (ε). The investigated dye (7–10 mg) was dissolved in buffer (50 mL), the stock solution was diluted to the dye concentration c_{Dye} ~ 1 μM and the absorbance (A) in the absorption band maximum was measured in a 5-cm standard quartz cell. The molar absorptivities were calculated according to the Beer-Lambert law. The molar absorptivity of each dye was independently measured three times and the average value was taken. The reproducibility for determining the molar absorptivity was within ± 200 $M^{-1}cm^{-1}$.

Fluorescence quantum yields (Φ_F) of the deprotonated dyes were measured *versus* rhodamine B (F_F = 71%) in ethanol as the reference using excitation wavelength λ_{ex} = 500 nm. The protonated dyes were measured versus coumarine 153 (F_F = 38%) in ethanol (λ_{ex} = 405 nm [33]. The absorbances of the samples and the references at the excitation wavelength were 0.04–0.08 measured in a 1-cm cell. The absolute

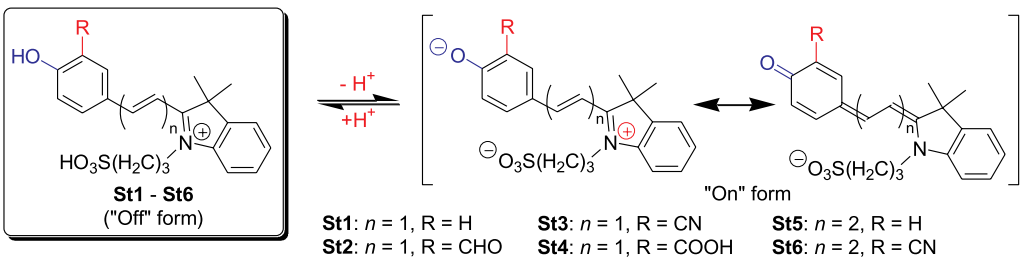

Scheme 2. Protonation-deprotonation of 2-(4-hydroxystyryl)- (n = 1) and 4-hydroxyphenyl-butadienyl (n = 2) indolenine dyes and resonance structures of the deprotonated forms.

quantum yields were calculated according to Equation (1) [33].

$$\Phi_F = \Phi_{FRef} \times (F / F_{Ref}) \times (A_{Ref} / A) \times (n_{D(water)}^2 / n_{D(EtOH)}^2), \quad (1)$$

where Φ_{FRef} is the quantum yield of the reference, F_{Ref} and F are the areas (integral intensities) of the emission spectra ($F = \int I(\lambda)d\lambda$) of the reference and the dye under examination, A_{Ref} and A are the absorbencies at the excitation wavelength of the reference and the dye under examination, and $n_{D(EtOH)}$ and $n_{D(water)}$ are the refractive indices of ethanol and water.

The quantum yield of each sample was independently measured 3–4 times and the average value was taken.

Brightness (B) was calculated as the molar absorptivity (ε) multiplied by the fluorescence quantum yields (Φ_F) expressed in fractions of a unit.

Acid-ionization constants (pK$_a$) were determined from both the absorption and emission titration curves using the non-linear fitting method expressed by Equations (2) and (3) [34].

$$pK_a(Abs) = pH - \log[\frac{(A_{max} - A)}{(A - A_{min})}], \quad (2)$$

where A_{max} and A_{min} are the absorbencies of the fully protonated and the deprotonated dye forms; A is the absorbance at a certain pH for the same dye concentration.

$$pK_a(Fl) = pH - \log[\frac{(I_{max} - I)}{(I - I_{min})}], \quad (3)$$

where I_{max} and I_{min} are the fluorescence intensities of the fully protonated and the deprotonated dye; I is the fluorescence intensity at a certain pH for the same dye concentration.

The pK_a of dyes **St1**–**St6** were measured at 1 μM dye concentration in buffer solutions of different pH. The following buffer solutions were used: (a) KCl/HCl covering the pH range 1.0–2.0; (b) AcOH/AcONa for the pH range 3.0–5.0; (c) NaH_2PO_4/Na_2HPO_4 for the pH range 6.0–8.0; (d) $NaHCO_3/Na_2CO_3$ for the pH range 9.2–10.8, (e) Na_2HPO_4/NaOH for the pH range 11.0–11.9, and (f) KCl/NaOH for the pH range 12.0–14.0. All of these buffer solutions were prepared with the same ionic strength (I_{st} = 0.1 M). The pH of the buffers was measured with a glass electrode (HANNA HI-2211 pH-meter) at 25 °C. The stock solutions of the compounds were prepared at 10 mM concentration in DMSO. Then the appropriate aliquots of the stock solutions were taken in 1-cm quartz cells equipped with screwed stoppers and diluted with buffer solution so that the absorbance in the maximum was 0.05–0.08. Each experiment was carried out in triplicate and the average values were taken.

pH sensing range was estimated as a pH region, where the absorption and fluorescence intensities change between 0.1 and 0.9 of the normalized value [35].

Chemical stability and drug release rates were measured spectrophotometrically and spectrofluorimetrically. For the chemical stability measurements, the samples were incubated in PB pH 7.4 at 37 °C. For the measurements of the drug release rates, the samples were incubated in PB pH 7.4 and CM pH 7.4 at 37 °C. All the spectral measurements were carried out at 25 °C. The absorption and fluorescence spectra for both chemical stability and drug release experiments were measured at ~1 μM compound concentration in certain time period and the corresponding graphs of the absorption and emission intensities *vs.* time were obtained. The half-lives ($\tau_{1/2}$) were calculated from the obtained exponential curves. Each experiment was carried out in triplicate and the average values were taken.

2.2. Synthesis

3-(2,3,3-Trimethyl-3*H*-1-indoliumyl)-1-propanesulfonate (2) was synthesized according to Ref. [18]. Yield 5.4 g (89%). ^{1}H NMR (400 MHz, DMSO-d_6, ppm): δ 8.05 (dd, J = 5.6, 3.2 Hz, 1H), 7.65–7.54 (m, 2H), 4.65 (t, 2H), 2.83 (s, 3H), 2.64 (dd, J = 8.5, 4.5 Hz, 2H), 2.21–2.10 (m, J = 14.4, 7.1 Hz, 2H), 1.53 (s, 6H). MS m/z (El+) $C_{14}H_{19}NO_3S^+$ calculated $[M+H]^+$ 282.7, found: 282.9.

2-(4-Hydroxystyryl)-3,3-dimethyl-1-(3-sulfopropyl)-3*H*-indolium (St1): To a solution of idolenine **Ind** (0.36 mmol, 100 mg) in AcOH (2 mL), the 4-hydroxybenzaldehyde (0.43 mmol, 53 mg) and AcONa (0.54 mmol, 44 mg) were added and refluxed for 30 min. The reaction was monitored by TLC. After the reaction was completed, the solution was diluted with Et_2O (50 mL) and cooled to RT. The obtained solid was filtered, dissolved in CH_3CN—H_2O (5:3, v.v.) and purified by HPLC. Yield 33 mg (42%). ^{1}H NMR (400 MHz, DMSO-d_6) δ 8.40 (d, J = 16.0 Hz, 1H), 8.20 (d, J = 8.7 Hz, 2H), 7.94 (d, J = 7.2 Hz, 1H), 7.83 (dd, J = 7.2, 1.2 Hz, 1H), 7.69 (d, J = 16.0 Hz, 1H), 7.62–7.53 (m, 2H), 6.94 (d, J = 8.8 Hz, 2H), 4.79 (t, J = 8.0 Hz, 2H), 2.65 (t, J = 6.0 Hz, 2H), 2.20–2.10 (m, 2H), 1.78 (s, 6H). ^{13}C NMR (100 MHz, DMSO-d_6) δ 174.73, 159.30, 154.79, 140.76, 140.03, 129.98, 129.98, 128.49, 127.62, 125.45, 122.88, 116.37, 116.37, 114.69, 106.17, 49.12, 48.51, 41.80, 26.14, 26.14, 23.14. HRMS m/z (El^+) $C_{21}H_{24}NO_4S^+$ calculated $[M+H]^+$ 386.1426, found 386.1417.

2-(3-Formyl-4-hydroxystyryl)-3,3-dimethyl-1-(3-sulfopropyl)-3*H*-indolium (St2): Dye **QCy7** (50 mg) was dissolved in 25% aq. NaOH (2 mL) and kept at RT for 30 min. The obtained dark-purple solution was purified by HPLC to give **St2.** Yield 15 mg (50%). ^{1}H NMR (400 MHz, DMSO-d_6) δ 8.26 (d, J = 15.0 Hz, 1H), 8.18 (d, J = 8.8 Hz, 2H), 7.66 (d, J = 7.4 Hz, 2H), 7.45 (t, J = 7.6 Hz, 1H), 6.45 (d, J = 8.5 Hz, 1H), 4.51 (s, 2H), 2.59 (t, J = 6.4 Hz, 2H), 2.05 (d, J = 1.4 Hz, 2H), 1.21 (s, 1H). ^{13}C NMR (100 MHz, DMSO-d_6) δ 154.04, 153.94, 153.69, 142.04, 141.48, 128.59, 126.60, 126.25, 125.62, 122.56, 119.75, 112.58, 112.42, 62.78, 49.96, 47.43, 43.22, 29.17, 26.69, 23.74. HRMS m/z (El^+) $C_{22}H_{24}NO_5S^+$ calculated $[M+H]^+$ 414.1375, found 414.1367.

5-Formyl-2-hydroxybenzonitrile (4). The synthesis was performed according to Ref. [36]. Yield 196 mg (40%). Purity: 89% (LC-MS, 254 nm). MS m/z (El^-) $C_8H_4NO_2^-$ calculated $[M-H]^-$ 146.1, found: 145.8.

2-(3-Cyano-4-hydroxystyryl)-3,3-dimethyl-1-(3-sulfopropyl)-3*H*-indolium (St3): The synthesis was performed according to Ref. [36]. Yield 63 mg (42%). ^{1}H NMR (400 MHz, DMSO-d_6) δ 8.58 (d, J = 2.1 Hz, 4H), 8.51 (dd, J = 8.9, 2.2 Hz, 4H), 8.38 (d, J = 16.3 Hz, 4H), 7.99 (dd, J = 6.1, 2.7 Hz, 4H), 7.88–7.81 (m, 4H), 7.77 (d, J = 16.3 Hz, 4H), 7.66–7.55 (m, 8H), 7.15 (d, J = 8.9 Hz, 4H), 5.72 (s, 1H), 4.90–4.75 (m, 9H), 2.73–2.63 (m, 9H), 2.23–2.10 (m, 8H), 1.77 (s, 25H), 1.22 (s, 4H). ^{13}C NMR (100 MHz, DMSO-d_6) δ 152.00, 137.53, 136.34, 129.13, 128.97, 122.85, 116.93, 114.91, 111.15, 97.23, 46.97, 45.25, 39.92, 39.71, 39.50, 39.29, 39.08, 25.45, 24.37. HRMS m/z (El^+) $C_{22}H_{23}N_2O_4S^+$ calculated $[M+H]^+$ 411.1379, found 411.1377.

2-(3-Carboxy-4-hydroxystyryl)-3,3-dimethyl-1-(3-sulfopropyl)-3H-indolium (St4): The solution of **St3** (0.08 mmol, 34 mg) in 48% aq. HBr (5 mL) was refluxed overnight and evaporated under low pressure. The resulted solid was filtered, dissolved in CH_3CN—H_2O (5:3, v.v.) and purified by HPLC. Yield 15 mg (42%). ^{1}H NMR (400 MHz, DMSO) δ 8.68 (d, J = 2.0 Hz, 1H), 8.65 (dd, J = 4.0, 2.2 Hz, 1H), 8.52 (d, J = 16.4 Hz, 1H), 8.02–7.97 (m, 1H), 7.87–7.84 (m, 1H), 7.78 (d, J = 16.4 Hz, 1H), 7.64–7.56 (m, 2H), 7.13 (d, J = 8.7 Hz, 1H), 4.84 (t, J = 8.0 Hz, 2H), 2.65 (d, J = 6.4 Hz, 2H), 2.21–2.12 (m, 2H), 1.80 (s, 6H). ^{13}C NMR (100 MHz, DMSO-d_6) δ 181.79, 171.08, 165.32, 158.40, 158.02, 153.53, 143.76, 140.79, 136.94, 135.45, 129.04, 126.24, 122.94, 118.67, 114.95, 114.15, 113.88, 110.74, 52.01, 47.16, 45.27, 25.61, 24.58. HRMS m/z (El^+) $C_{22}H_{24}NO_6S^+$ calculated $[M+H]^+$ 430.1324, found 430.1327.

4-Methoxybenzaldehyde (7): The synthesis was performed according to Ref. [37]. Yield 2.15 g (63%). MS m/z (El^+) $C_8H_8O_2^+$ calculated $[M+H]^+$ 137.7, found: 137.1.

3-(4-Methoxyphenyl)acrylaldehyde (9): The synthesis was carried out according to Ref. [38]. Yield 90 mg (15%). MS m/z (El^+) $C_{10}H_{10}O_2^+$ calculated $[M+H]^+$ 162.2, found: 162.1.

4-(4-Methoxyphenyl)buta-1,3-dienyl)-3,3-dimethyl-1-(3-sulfopropyl)-3*H*-indolium (St5-Me): Indolenine **2** (5 mmol, 0.145 g) was dissolved in Ac_2O (1.5 mL) and 4-methoxyphenylacrylaldehyde **9** (6 mmol, 0.1 g) was added. The reaction mixture was brought to the reflux. Then, AcONa (7.5 mmol, 0.62 g) was added to the boiled mixture was refluxed for additional 30 min. The reaction was monitored by TLC. After the reaction was completed, the solution was diluted with Et_2O (25 mL) and cooled to RT. The obtained solid was filtered, dissolved in CH_3CN—H_2O (1:1, v.v.) and purified by HPLC. Yield 22 mg (22%). ^{1}H NMR (400 MHz, MeOH-d_4) δ 8.34 (dd, J = 15.1, 10.9 Hz, 1H), 7.87 (d, J = 7.2 Hz, 1H), 7.76–7.70 (m, 3H), 7.67–7.55 (m, 3H), 7.42 (dd, J = 15.1, 10.9 Hz, 1H), 7.26 (d, J = 15.1 Hz, 1H), 7.03 (d, J = 8.8 Hz, 2H), 4.73 (ABq, 2H), 3.88 (s, 3H), 3.04 (t, J = 6.5 Hz, 2H), 2.40–2.30 (m, 2H), 1.81 (s, 6H). ^{13}C NMR (100 MHz, MeOH-d4) δ 175.69, 159.94, 154.08, 140.76, 140.03, 136.92, 129.44, 128.75, 128.75, 128.49, 127.63, 125.45, 122.88, 114.69, 114.58, 114.58, 108.61, 56.04, 49.12, 48.51, 41.80, 26.14, 26.14, 23.14. HRMS m/z (El^+) $C_{24}H_{28}NO_4S^+$ calculated $[M+H]^+$ 427.1739, found: 426.1730.

4-(4-Hydroxyphenyl)buta-1,3-dienyl)-3,3-dimethyl-1-(3-sulfopropyl)-3H-indolium (St5): To a solution of **St5-Me** (0.122 mmol, 52 mg) in dichloromethane (5 mL) a solution of boron tribromide (3 mmol, 300 µl) in dichloromethane (2 mL) was carefully added during 2 min. The reaction mixture was stirred at room temperature for 30 min, solvent evaporated and the residue purified by HPLC. Yield 45 mg (85%). ^{1}H NMR (400 MHz, MeOH-d_4) δ 8.92 (s, 1H), 8.33 (dd, J = 15.0, 11.0 Hz, 1H), 7.84 (d, J = 7.3 Hz, 1H), 7.71 (d, 1H), 7.65 (d, J = 8.6 Hz, 2H), 7.61–7.54 (m, 3H), 7.38 (dd, J = 15.1, 11.0 Hz, 1H), 7.22 (d, 1H), 6.88 (d, J = 8.7 Hz, 1H), 4.71 (ABq, 2H), 3.03 (t, J = 6.5 Hz, 2H), 2.39–2.29 (m, 2H), 1.80 (s, 6H). ^{13}C NMR (100 MHz, MeOH-d4) δ 175.69, 158.47, 154.08, 140.76, 140.03, 136.92, 129.38, 129.38, 128.49, 128.39, 127.63, 125.45, 122.88, 116.38, 116.38, 114.69, 108.61, 49.12, 48.51, 41.80, 26.14, 26.14, 23.14. HRMS m/z (El^+) $C_{23}H_{26}NO_4S^+$ calculated $[M+H]^+$ 412.1583, found 412.1581.

5-Formyl-2-methoxybenzonitrile (4): The synthesis was performed according to Ref. [37]. Yield 12 mg (24%). MS m/z (El^-) $C_9H_7NO_2^-$ calculated $[M-H]^-$ 160.8, found: 160.1.

2-Methoxy-5-(3-oxoprop-1-enyl)benzonitrile (10): The synthesis was carried out according to Ref. [38]. Yield 75 mg (30%). MS m/z (El^+) $C_{11}H_9NO_2^+$ calculated $[M-H]^+$ 187.2, found: 187.1.

4-(3-Cyano-4-methoxyphenyl)buta-1,3-dienyl)-1-(3-(mercaptotrioxidanyl)propyl)-3,3-dimethyl-3H-indolium (St6-Me): Indolenine **2** (1.3 mmol, 0.370 g) was dissolved in AcOH (3 mL) and after addition of benzonitrile **10** (6 mmol, 0.1 g) the reaction mixture was brought to the reflux. Then, AcONa (7.5 mmol, 0.62 g) was added to the boiled mixture and refluxed for additional 30 min. The reaction was monitored by TLC. After completion of the reaction, the reaction mixture was diluted with Et_2O (25 mL) and cooled to RT. The obtained precipitate was filtered, dissolved in CH_3CN—H_2O (1:1, v.v.) and purified by HPLC. Yield 0.187 mg (21%). ^{1}H NMR (400 MHz, DMSO-d_6) δ 8.35 (d, J = 15.1 Hz, 1H), 8.09 (s, 1H), 8.00 (s, 2H), 7.85 (s, 1H), 7.70 (s, 1H), 7.68 (s, 1H), 7.61 (s, 2H), 7.40 (d, J = 9.1 Hz, 1H), 4.67 (s, 2H), 4.00 (s, 4H), 2.64 (s, 2H), 2.14 (s, 2H), 1.74 (s, 5H). ^{13}C NMR (100 MHz, DMSO-d_6) δ 175.69, 162.56, 154.08, 140.76, 140.03, 137.09, 134.05, 133.43, 131.04, 128.64, 128.49, 125.45, 122.88, 115.94, 114.69, 111.30, 108.61, 97.34, 56.79, 49.12, 48.51, 41.80, 26.14, 26.14, 23.14. HRMS m/z (El^+) $C_{25}H_{27}N_2O_4S^+$ calculated $[M-H]^-$ 451.1692, found: 451.1694.

4-(3-Cyano-4-hydroxyphenyl)buta-1,3-dienyl)-1-(3-(mercaptotrioxidanyl)propyl)-3,3-dimethyl-3*H*-indolium (St6): To a solution of **St2-Me** (0.067 mmol, 30 mg) in dichloromethane (2 mL) was carefully added a solution of boron tribromide in dichloromethane (1.2 mmol, 1.2 mL) during 2 min. The reaction mixture was stirred at room temperature for 30 min, solvent evaporated and the residue purified by HPLC. Yield 24 mg (80%). ^{1}H NMR (400 MHz, DMSO-d_6) δ 11.96 (s, 1H), 8.34 (dd, J = 15.2, 10.7 Hz, 1H), 7.98 (dd, J = 8.3, 4.7 Hz, 2H), 7.88–7.82 (m, 2H), 7.61 (ddd, J = 17.5, 13.4, 11.3 Hz, 3H), 7.42–7.30 (m, 2H), 7.13 (d, J = 8.8 Hz, 1H), 4.74–4.59 (m, 2H), 2.63 (t, J = 6.8 Hz, 2H), 2.14 (dd, J = 14.6, 6.9 Hz, 2H), 1.74 (s, 6H). ^{13}C NMR (100 MHz, DMSO-d_6) δ 175.69, 161.81, 154.08, 140.76, 140.03, 137.09, 134.65, 132.71, 131.31, 128.64, 128.49, 125.45, 122.88, 115.38, 114.69, 114.69, 108.61, 94.20, 49.12, 48.51, 41.80, 26.14, 26.14, 23.14. HRMS m/z (El^+) $C_{24}H_{25}N_2O_4S^+$ calculated $[M-H]^+$ 437.1535, found: 437.1537.

2-(4-(4-(4-(4-(bis(2-chloroethyl)amino)phenyl)butanoyloxy)-3-cyanophenyl)buta-1,3-dienyl)-3,3-dimethyl-1-(3-sulfopropyl)-3H-indolium (St6-CLB): Chlorambucil (0.024 mmol, 7.3 mg) and DCC (0.048 mmol, 10 mg) were stirred in NMP at RT for 10 min. Then **St6** (0.012 mmol, 5 mg) and pyridine (2 µL) were sequentially added and the reaction mixture was stirred for additional 1.5 h at RT. The reaction was monitored by TLC. After completion of the reaction, the solution was diluted with Et_2O (25 mL), the obtained solid was filtered, dissolved in CH_3CN—H_2O (1:1, v.v.) and purified by HPLC. Yield 2 mg (23%). ^{1}H NMR (400 MHz, DMSO-d_6) δ 8.43 (s, 4H), 7.57 (d, J = 7.5 Hz, 4H), 7.48 (d, J = 7.2 Hz, 4H), 7.33 (d, J = 8.8 Hz, 4H), 7.17 (d, J = 7.5 Hz, 4H), 6.95–6.87 (m, 12H), 6.77 (d, J = 15.3 Hz, 4H), 6.67–6.55 (m, 12H), 4.51 (s, 8H), 3.70 (s, 16H), 3.55 (s, 16H), 3.16 (s, 8H), 2.63 (s, 8H), 2.53 (s, 8H), 2.29 (s, 3H), 2.25 (s, 3H), 1.90 (s, 7H), 1.44 (s, 24H). ^{13}C NMR (100 MHz, DMSO-d_6) δ 175.69, 173.14, 156.49, 154.08, 146.56, 140.76, 140.03, 137.09, 135.02, 134.06, 132.73, 130.27, 130.27, 129.43, 128.64, 128.49, 125.45, 122.88, 120.53, 115.94, 115.22, 115.22, 114.69, 108.61, 102.71, 50.96, 50.96, 49.12, 48.51, 41.88, 41.88, 41.80, 35.85, 33.39, 26.14, 26.14, 24.39, 23.14. HRMS m/z (El^+) $C_{38}H_{42}Cl_2N_3O_5S+$ calculated $[M+H]^+$ 722.2222, found: 723.2297.

3. Results and discussion

3.1. Synthesis

Styryl dye **St1** was previously reported in Ref. [18]. We synthesized this dye in 42% yield by the condensation of 4-hydroxybenzaldehyde (**1**) with the quaternized indolenine **2** (Scheme 3). The last one was obtained by the quaternization of indolenine **3** with 1,3-propane sultone.

The new dye **St2** was synthesized by alkaline hydrolysis of cyanine **QCy7** (Scheme 4) similar to the method described in Ref. [39]. The known procedure was improved by using 25% aq. NaOH instead of 100 mM phosphate buffer (pH 7.4), which allowed decreasing the reaction time from 10 days to 30 min.

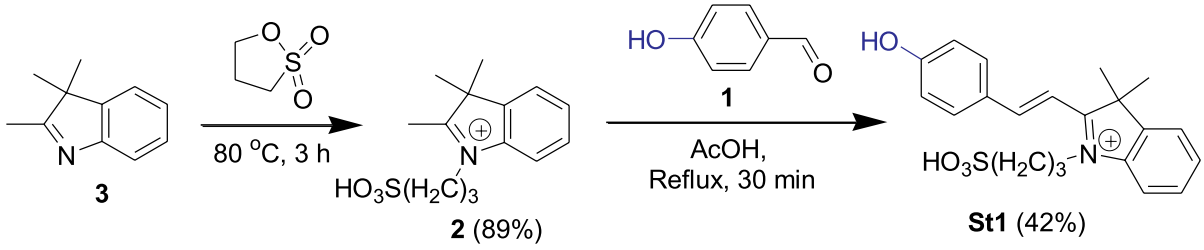

Scheme 3. Synthesis of dye **St1**.

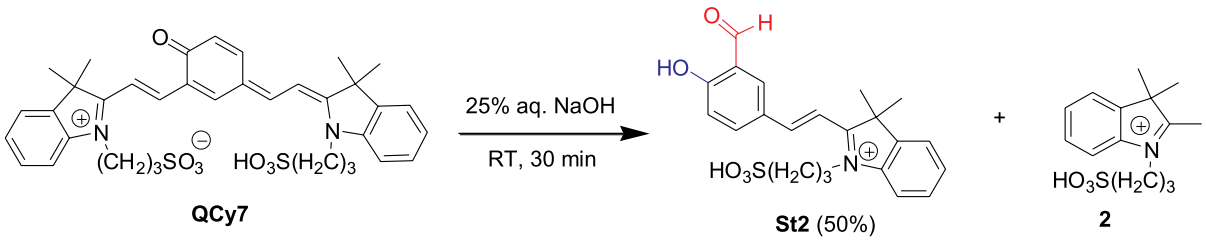

Scheme 4. Synthesis of 3-formyl-styryl dye **St2**.

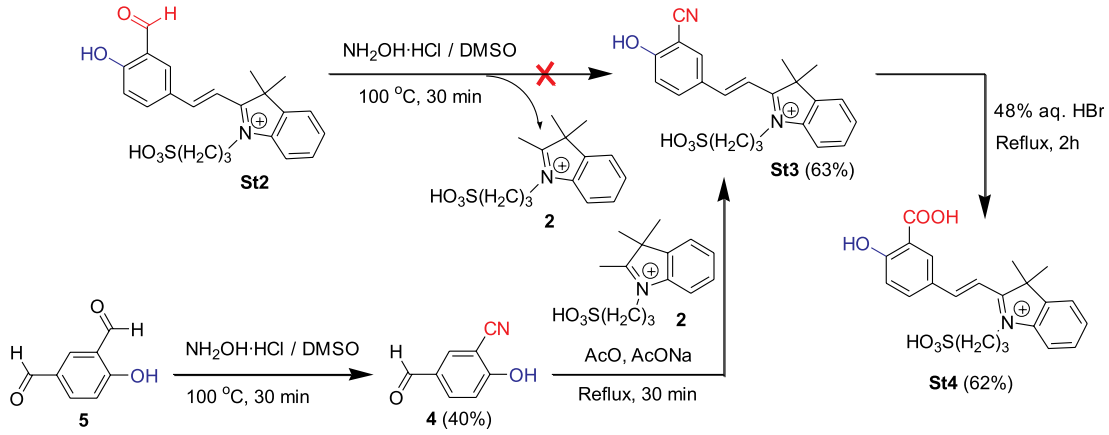

Scheme 5. Synthesis of 3-cyano and 3-carboxy styryls **St3** and **St4**.

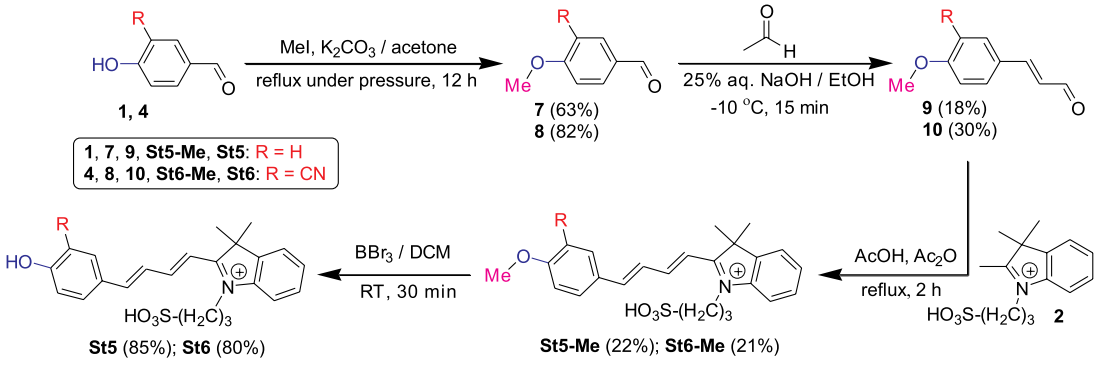

Scheme 6. Synthesis of 4-hydroxyphenyl-butadienyl dyes **St5-Me**, **St5**, **St6-Me**, and **St6**.

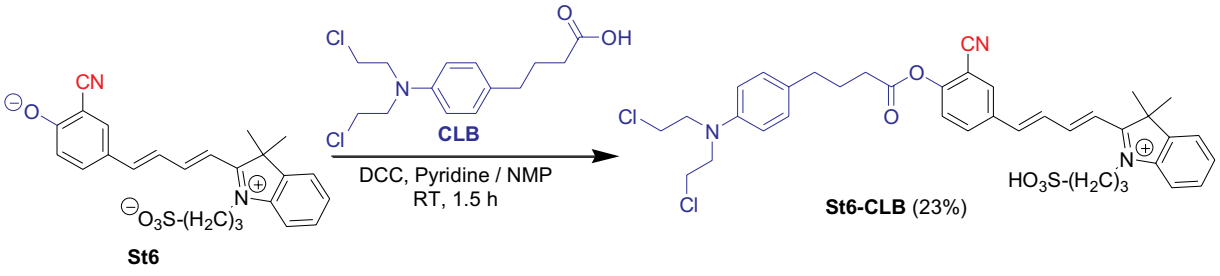

Scheme 7. Synthesis of **St6–CLB** conjugate.

Attempts to synthesize the nitrile dye **St3** starting from the formylated dye **St2** by using the procedure [36] have failed since **St2** decomposed to indolenine **2** (37% yield) and a mixture of other, non-identified products (Scheme 5). Therefore, dye **St3** was synthesized by condensation of indolenine **2** with 3-cyano-4-hydroxybenzaldehyde (**4**). The last one was obtained by a reaction of dialdehyde **5** with hydroxylamine in DMSO. Aldehyde **4** was reacted with **2** in acetic anhydride to form **St3** in 63% yield (Scheme 5). The carboxylated dye **St4** was obtained in 62% yield by hydrolysis of cyano group in **St3** under reflux with 48% aq. HBr (Scheme 4).

Dyes **St5** and **St6** were synthesized starting from 4-hydroxybenzaldehydes **1** and **4** as shown in Scheme 6. By using methyl iodide [37], a hydroxyl group in **1** and 4 was protected with a methyl to form 4-methoxybenzaldehydes **7** and **8** that were reacted with acetaldehyde

Table 1
Spectral and protolytic characteristics of styryl dyes **St1–St6** in the protonated (OH) and deprotonated (O^-) forms.

Parameter	Dye											
	$n = 1$						$n = 2$					
	St1 (R = H)		St2 (R = CHO)		St3 (R = CN)		St4 (R = COOH)		St5 (R = H)		St6 (R = CN)	
	OH	O^-	OH	O^-	OH	O^-	OH	O^-	OH	O^-	OH	O^-
λ_{max}Ab ($\Delta\lambda$[a]), nm	428	529	414	501	411	493	433	536	469 (41)	603 (74)	444 (33)	536 (43)
λ_{max}Fl ($\Delta\lambda$[a]), nm	530	554	–[b]	558	–[b]	554	548	558	613 (83)	658 (107)	–[b]	653 (99)
$\omega_{1/2}$Ab, cm^{-1}	4740	2600	5350	3520	4850	3560	4720	2340	4720	3580	5010	4760
$\omega_{1/2}$Fl, cm^{-1}	4440	1430	–[b]	1540	–[b]	1810	2530	1600	2700	1150	–[b]	1460
$\Delta\nu_{St}$, cm^{-1}	4500	850	–[b]	1890	–[b]	2270	6650	790	5000	1390	–[b]	3340
ε, $M^{-1}cm^{-1}$	31,900	62,500	27,400	43,300	27,400	41,200	28,700	59,900	27,800	35,740	17,470	19,520
Φ_F, %	0.21 ± 0.02	0.37 ± 0.01	–[b]	1.22 ± 0.02	–[b]	1.23 ± 0.02	0.39 ± 0.02	0.77 ± 0.03	1.53 ± 0.02	1.81 ± 0.03	–[b]	6.47 ± 0.04
B, $M^{-1}cm^{-1}$	70	230	–[b]	530	–[b]	510	110	460	425	650	–[b]	1260
pK_a ± SD (absorption, emission)	6.96 ± 0.09		5.93 ± 0.28		4.67 ± 0.18		9.93 ± 0.10		7.98 ± 0.12		5.57 ± 0.10	
	7.10 ± 0.01		5.83 ± 0.32		4.61 ± 0.21		9.76 ± 0.12		7.89 ± 0.05		5.54 ± 0.12	
pH range (absorption, emission)	5.9–9.3		4.7–6.9		3.1–6.4		8.5–11.2		7.1–9.2		4.1–6.7	
	6.0–9.0		4.4–7.0		3.1–6.4		8.9–11.6		6.6–8.9		3.8–6.8	

[a] $\Delta\lambda$ is a spectral shift for 4-hydroxyphenyl-butadienyl dye ($n = 2$) compared to 4-hydroxystyryl dye ($n = 1$) with the same substituent R.
[b] No detectable fluorescence.

to give cinnamaldehydes **9** and **10**, correspondingly. The last ones were condensed with indolenine **2** to the methoxylated dyes **St5-Me** and **St6-Me**, which were further demethylated with BBr_3 to form the aimed hydroxylic dyes **St5** and **St6**, respectively, in good yields.

To examine the applicability of dye **St6** as an "Off-On" switchable reporter in drug delivery monitoring, this dye was bound to the anticancer drug chlorambucil (CLB) acting as DNA alkylator [40]. Thus, CLB was pre-activated with DCC and reacted with **St6** to give the **St6–CLB** conjugate in 23% yield. The reaction was carried out in mild conditions at RT (NMP with a catalytic amount of pyridine) (Scheme 7). As a result, the drug was bound to the dye *via* a hydrolytically cleavable ester bond, which is commonly used in the drug and prodrug delivery in biological systems [41,42].

3.2. Spectral properties

Spectral properties of dyes **St1–St6** were measured in 0.1 M buffer solutions of different acidity. The absorption and emission maxima (λ_{max}Ab, λ_{max}Fl), spectral half-widths ($\omega_{1/2}$Abs, $\omega_{1/2}$Fl), Stokes shifts ($\Delta\nu_{St}$), molar absorptivities (ε), fluorescence quantum yield (Φ_F), and brightness (B) of the protonated (OH) and deprotonated (O^-) forms of the dyes are summarized in Table 1.

Due to the presence of the sulfo group, all the investigated dyes **St1**–**St6** are well soluble in water and aqueous buffer solutions, which is important for their practical applications. Thus, the absorption spectra of these dyes do not exhibit any signs of aggregation: there is no additional, aggregation band and the Beer–Lambert law is valid in the investigated concentration range at least up to 10^{-5} M.

Dyes **St1–St4** absorb in the blue-green and emit in the green-yellow spectral region while the spectral bands of **St5** and **St6** are noticeably red-shifted by about 33–74 nm for absorption ($\Delta\lambda_{Ab}$) and 83–107 nm for emission ($\Delta\lambda_{Fl}$). As a result, **St5** and **St6** absorb in the green-yellow and emit in the red region, which is more attractive for probing in biological samples.

The introduction of the electron-withdrawing formyl (**St2**) and cyano (**St3**, **St6**) groups in the *ortho* position to the hydroxyl functionality (**St1**, **St5**) causes a blue-shift of the absorption maximum for both protonated and deprotonated forms while a slight red-shift is observed upon the introduction of the carboxylic group (**St4**). The different behavior of the carboxylic group is connected more likely with the formation of an intramolecular *H*-bond with the 4-hydroxyl group; the *H*-bonding with the water molecules might also be responsible for this effect [43].

The molar absorptivities of the deprotonated forms of **St1–St6** are 1.5–2.1-fold higher compared to those for the protonated forms while for **St5** and **St6** this increase is less pronounced, 1.1–1.3 time. The protonated forms of **St2**, **St3** and **St6** (R = CHO, CN) show no detectable fluorescence. At the same time, both protonated and deprotonated forms of **St1**, **St4** and **St5** (R = H, COOH) are fluorescent and the fluorescence quantum yields of the deprotonated dyes are 1.2–2.0 fold higher compared to the protonated forms.

In general, the fluorescence quantum yields of previously reported 4-hydroxystyryl dyes measured in polar solvents are poor, which is typical for any donor-acceptor systems. Nevertheless, these dyes were proposed for many practical applications due to their extreme sensitivity to analytes [16,18,23]. The quantum yield of **St1** is in agreement with recently reported data on the styryl dyes of similar structure [44]. Importantly, the introduction of the electron-withdrawing formyl, cyano and carboxyl groups noticeably increases the quantum yield of the deprotonated forms by factor of 2.1–3.6 (Table 1). In addition, the extension of π-conjugated system ($n = 2$ *versus* $n = 1$) also increases the quantum yield of **St5** compared to **St1** by factor of 4.9 and by factor of 5.3 for **St6** *versus* **St3**. As a result, the quantum yield of the deprotonated form of **St6** is about 17.5 fold higher compared to **St1**. For protonated form of **St1** the quantum yield also increases upon the introduction of the carboxylic group (dye **St4**) but this increase is not

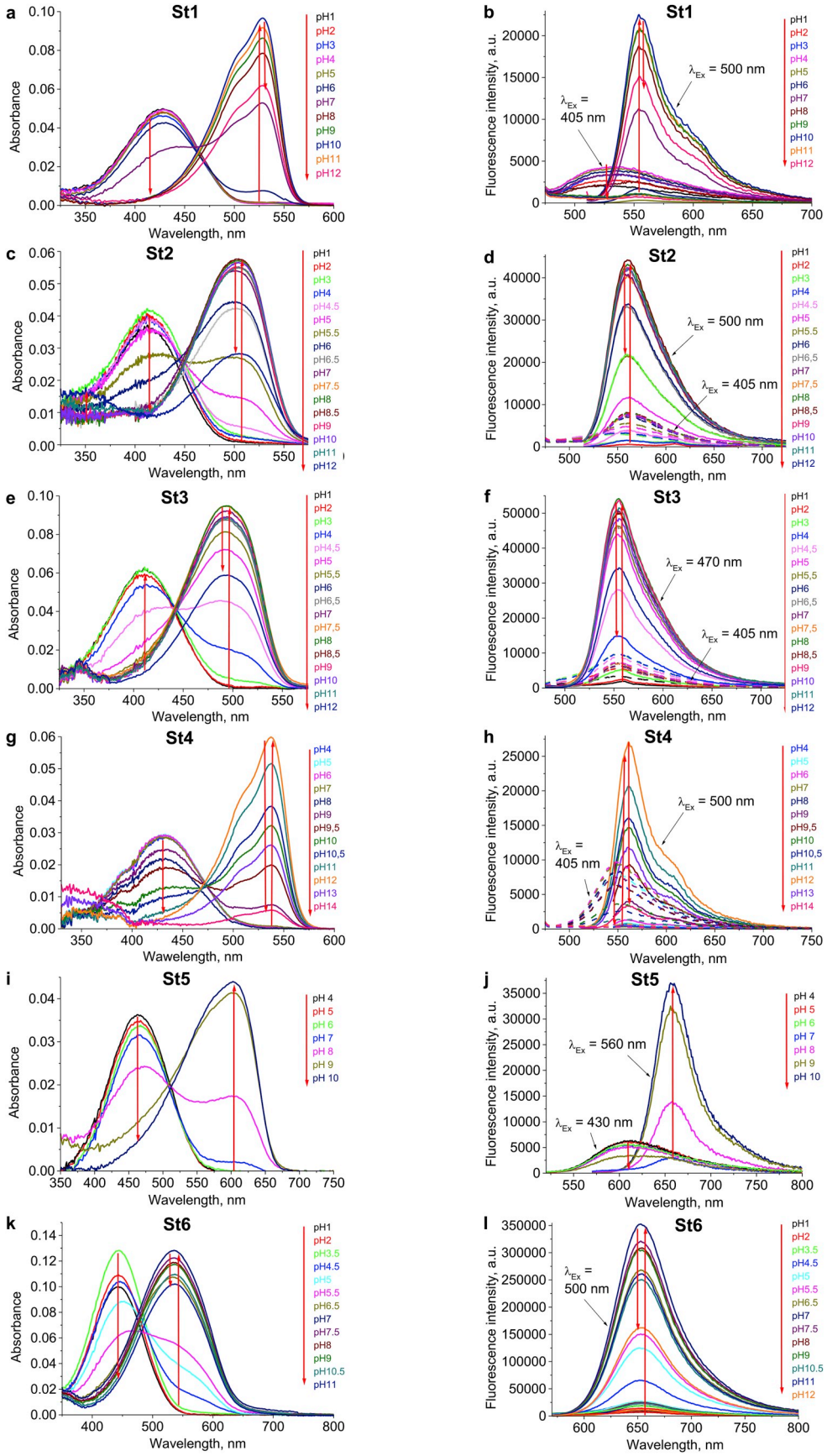

Fig. 1. pH-Dependent absorption (***a, c, e, g, i, k***) and fluorescence (***b, d, f, h, j, l***) spectra of **St1** (***a***, ***b***), **St2** (***c***, ***d***), **St3** (***e***, ***f***), **St4** (***g***, ***h***), **St5** (***i***, ***j***), and **St6** (***k***, ***l***). λ_{Ex}(protonated forms): 405 nm for **St1–St4**; 430 nm for **St5**. λ_{Ex}(deprotonated forms): 500 nm for **St1**, **St2**, **St4**, and **St6**; 470 nm for **St3** and 560 nm for **St5**.

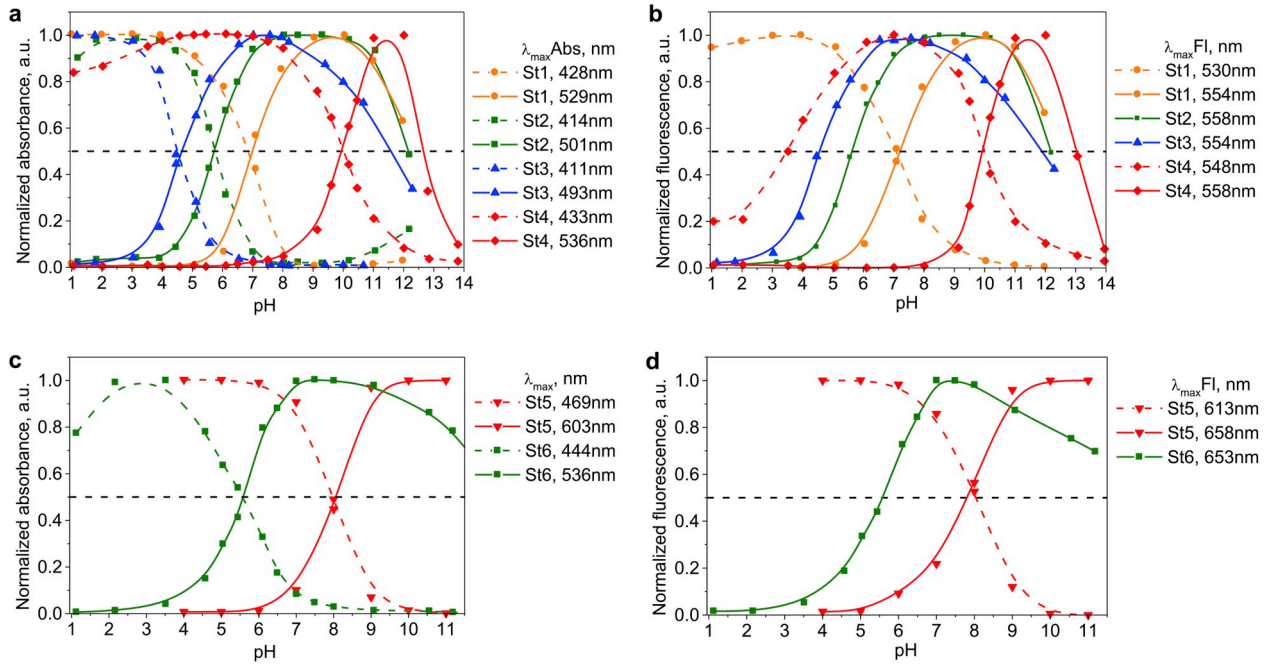

Fig. 2. Titration curves for **St1–St4** (***a***, ***b***), **St5** and **St6** (***c***, ***d***) in the protonated (dashed line) and deprotonated (solid line) forms measured spectrophotometrically (***a***, ***c***) and spectrofluorimetrically (***b***, ***d***).

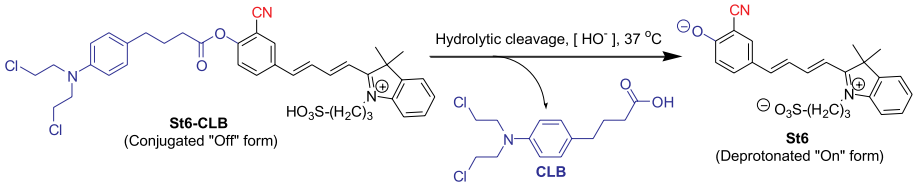

Scheme 8. Hydrolytic cleavage of CLB in the non-fluorescent **St6–CLB** conjugate to form fluorescent dye **St6** (deprotonated form).

pronounced (1.9 fold).

The deprotonated forms of **St1–St6** emit with relatively small Stokes shifts ($\Delta\nu_{St}$ ~ 850–3340 cm^{-1}) while for the protonated forms of **St1**, **St4** and **St5** $\Delta\nu_{St}$ noticeably increase by 5.3, 8.4 and 3.6 fold, respectively. The Stokes shifts for 4-hydroxyphenyl-butadienyl dyes **St5** and **St6** are a bit higher compared to 4-hydroxystyryls **St1** and **St3**, which is more likely due to the longer polymethine chain and increased conformational lability. The half-widths ($\omega_{1/2}$) of the absorption and emission bands of the deprotonated forms are always narrower than those for the protonated dyes.

In summary, the spectral properties of the deprotonated 4-hydroxystyryl and 4-hydroxyphenyl-butadienyl dyes containing the zwitterionic fluorophore system, as compared to the positively charged protonated forms (Scheme 2), are very similar to those for the positively charged cyanines and norcyanines and zwitterionic squaraines and norsquaraines [45–47]. These deprotonated forms are brighter (have higher Φ_F and ε), exhibit shorter Stokes shifts, and their absorption and emission spectral bands are red-shifted and narrower.

In addition, because the absorption bands of the dyes **St1**, **St4** and **St5** lie in the substantially different spectral regions and the emission maxima are also noticeably different, these dyes are potentially suitable for the ratiometric fluorescence sensing measurements, that have certain advantages in particular for quantitative measurements in biological systems [48].

3.3. Protolytic properties

The absorption and emission spectra of dyes **St1–St6** *versus* pH were measured in aqueous buffer solutions (Fig. 1) and the corresponding titration curves were obtained (Fig. 2). The emission spectra of the protonated and deprotonated forms were recorded under the excitation in the corresponding absorption bands. Based on the obtained spectrophotometric and spectrofluorimetric titration curves, the acid-ionization constants (pK_a) were calculated. The pK_a values found from the emission titration curves are very similar to those obtained spectrophotometrically (the difference is only 0.03–0.17 pK_a units), which evidences that no pronounced structural changes occur with the dye molecules in the excited state. In respect to the substituent R, the pK_a values change in a wide range between ~4.6 and ~9.9. The pK_a increase in the order **St3** (n = 1, R = CN) < **St6** (n = 2, R = CN) < **St2** (n = 1, R = CHO) < **St1** (n = 1, R = H) < **St5** (n = 2, R = CN) < **St4** (n = 1, R = COOH) (Table 1). The introduction of the cyano group decreases the acid-ionization constant by about 2.4 pK_a units while the extension of the π-conjugated chain (n = 2 *vs.* n = 1) slightly increases it by ~0.9 pK_a units. Although the carboxyl group is an electron-withdrawing substituent, it increases pK_a due to the intramolecular *H*-bond formation. Such effect was discussed in Ref. [49] for salicylic acid derivatives.

Among all the investigated dyes, **St6** seems most advantageous for biomedical sensing applications. This is due to the deprotonated form of this dye exhibits more pronounced brightness as compared to other dyes, longer absorption and emission maxima compared to **St1–St4** and wider pH range (lower pK_a) compared to the long-wavelength dye **St5**. We also found that **St6** has a reasonable chemical stability in PB pH 7.4 at 37 °C (Fig. S1). Therefore, we decided to evaluate **St6** as the switchable fluorescent reporter for the detection of drug release events.

3.4. Monitoring of drug release

The applicability of dye **St6** for monitoring of drug release was

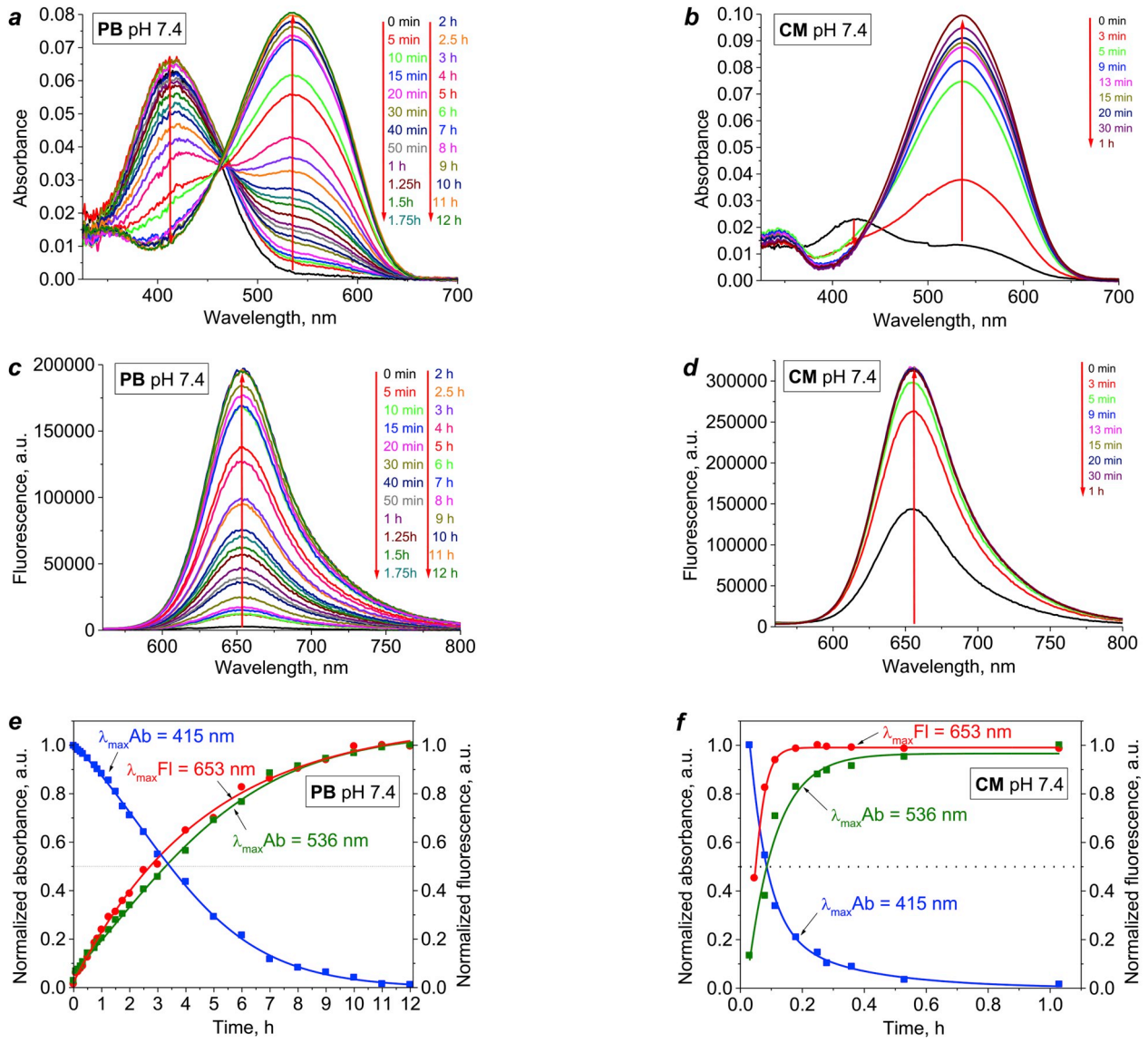

Fig. 3. Time dependent absorption (***a***, ***c***) and fluorescence (***b***, ***d***) spectra and the corresponding cleavage profiles (***e***, ***f***) of **St6-CLB** measured in PB (5 μM) pH 7.4 (***a***, ***c***, ***e***) and CM (5 μM) pH 7.4 (***b***, ***d***, ***f***) at 25 °C (incubation at 37 °C).

tested in the example of anticancer drug chlorambucil (CLB). In a hydrolytic environment, the ester bond in the **St6–CLB** conjugate was prone to cleavage releasing the drug molecule (Scheme 8). We investigated the spectral properties of **St6–CLB** and the CLB cleavage rate in physiological conditions (37 °C), in PB pH 7.4 and esterase containing cell culture medium pH 7.4 (CM).

The free **St6** is a pH-sensitive dye, which exists at pH 7.4 in the fluorescent deprotonated form (Fig. 3). The absorption (~536 nm) and emission (~653 nm) maxima in both PB and CM media are almost the same. The fluorescence intensity of **St6** in the protein containing CM is about 1.5 times higher compared to PB. Supposedly, this is due to the highly polar dye molecules in CM move from a polar aqueous media into a less polar and more viscous protein phase resulting in the decrease of non-radiative relaxation and the increase of the fluorescence quantum yield.

In contrast to the free **St6**, the CLB conjugated **St6** in both solvent systems behaves similar to the protonated **St6**: it absorbs at ~415 nm (a ~30-nm blue-shift compared to the protonated **St6**) and exhibits no detectible fluorescence.

The CLB cleavage was investigated using spectrophotometric and spectrofluorimetric methods. The time dependent absorption and emission spectra measured at the **St6-CLB** concentration ~1 μM and the corresponding cleavage profiles are shown in Fig. 3. It can be seen that in both media the absorption band at ~415 nm decreases over time and a new, longer-wavelength band at ~536 nm increases (Fig. 3a and b). Simultaneously, the fluorescence intensity dramatically increases signaling the CLB release (Fig. 3c and d). Due to the presence of esterases, hydrolytic cleavage in CM occurs about 45 times faster compared to PB. The CLB release half-life ($\tau_{1/2}$) in CM is about 4 min while in PB it is $\tau_{1/2}$–3 h (Fig. 3e and f). Because the cleavage in CM runs extremely fast, even the initial absorption and emission spectra of **St6–CLB** in CM show the presence of the free **St6** formed upon the CLB release.

3.5. Chemical stability

The stability of dyes plays an important role for their practical use. The stability of **St6** was investigated upon incubation in PB pH 7.4 at 37 °C. The absorption and emission spectra were measured at 25 °C over time (Figs. S1,a,b). The spectral bands related to the protonated form were found to decrease very slowly, by ~20% during 7 days (Figs. S1,c,d), which indicates that **St6** is sufficiently stable for conventional analytical and bioanalytical applications.

4. Conclusions

In summary, we have developed synthetic approaches to the novel, water-soluble 3-R-4-hydroxystyryl dyes **St1** (R = H), **St2** (R = CHO), **St3** (R = CN), and **St4** (R = COOH) and 3-R-4-hydroxyphenyl-butadienyl dyes **St5** (R = H) and **St6** (R = CN). These dyes were synthesized in satisfactory yields and their spectral and protolytic properties investigated in aqueous solutions.

All the dyes exhibit switchable fluorescence and pH-sensitivity between pH = 3.1–11.6 (pK_a ~4.6–9.9) in respect of the molecular structure. The extension of the π-conjugated system (4-hydroxyphenyl-butadienyls *versus* 4-hydroxystyryls) and the introduction of the electron-withdrawing formyl and cyano groups lead to a pronounced red-shift of the absorption and emission maxima (33–107 nm) and a considerable brightness increase for the deprotonated forms. The introduction of the formyl and cyano groups decreases the pK_a while the carboxylic group and the extension of the conjugated chain have the opposite effect. Unlike the protonated dyes, the deprotonated forms behave similar to cyanines, norcyanines, squaraines, and norsquaraines: they are brighter, exhibit shorter Stokes shifts and their spectral bands are red-shifted and narrower.

Dyes **St2**, **St3** and **St6** demonstrate "Off-On" activatable fluorescence; their brightness is higher compared to **St1**, **St4** and **St5** and the pK_a are lower, which makes these dyes beneficial for sensing applications. In contrast, both protonated and deprotonated forms of **St1**, **St4** and **St5** are fluorescent and therefore these dyes are potentially suitable for the dual-wavelength ratiometric fluorescence measurements. The new dyes can be used as acidity indicators within the physiological pH range. Due to its activatable long-wavelength fluorescence, low pK_a, high water-solubility, and chemical stability, dye **St6** is suitable as a "turn-on" activatable reporter for fluorescence monitoring of drug release events.

Acknowledgements

This research was supported by the Israel Scientific Foundation (ISF), project 810/18. Leonid Patsenker is thankful to the Center for Absorption in Science of the Ministry of Immigrant Absorption of Israel for the financial support under the KAMEA program. Gary Gellerman is thankful to the Gale Foundation for the generous donation to support this research.

Appendix A. Supplementary data

Supplementary data to this article can be found online at https://doi.org/10.1016/j.dyepig.2019.107801.

References

[1] Zhu H, Derksen R, Krause C, Fox R, Brazee R, Ozkan H. Fluorescent intensity of dye solutions under different pH conditions. J ASTM Int (JAI) 2005;5(6):1–7. https://doi.org/10.1520/JAI12926.
[2] Han J, Burgess K. Fluorescent indicators for intracellular pH. Chem Rev 2010;110(5):2709–28. https://doi.org/10.1021/cr900249z.
[3] Wu D, Chen L, Lee W, Ko G, Yin J, Yoon J. Recent progress in the development of organic dye based near-infrared fluorescence probes for metal ions. Coord Chem Rev 2018;354:74–97. https://doi.org/10.1016/j.ccr.2017.06.011.
[4] Bazylevich A, Patsenker L, Gellerman G. Exploiting fluorescein based drug conjugates for fluorescent monitoring in drug delivery. Dyes Pigments 2017;139:460–72. https://doi.org/10.1016/j.dyepig.2016.11.057.
[5] Tang Y, Liu Y, Cao A. Strategy for sensor based on fluorescence emission red shift of conjugated polymers: applications in pH response and enzyme activity detection. Anal Chem 2012;85(2):825–30. https://doi.org/10.1021/ac302840t.
[6] Liu J, Yin Z. A novel NIR-emissive probe with large Stokes shift for hypochlorite detection and imaging in living cells. Talanta 2019;196:352–6. https://doi.org/10.1016/j.talanta.2018.12.086.
[7] Hawe A, Sutter M, Jiskoot W. Extrinsic fluorescent dyes as tools for protein characterization. Pharm Res 2008;25(7):1487–99. https://doi.org/10.1007/s11095-007-9516-9.
[8] Haque A, Faizi MS, Rather JA, Khan MS. Next generation NIR fluorophores for tumor imaging and fluorescence-guided surgery: a review. Bioorg Med Chem 2017;25(7):2017–34. https://doi.org/10.1016/j.bmc.2017.02.061.
[9] Luo S, Zhang E, Su Y, Cheng T, Shi C. A review of NIR dyes in cancer targeting and imaging. Biomaterials 2011;32(29):7127–38. https://doi.org/10.1016/j.biomaterials.2011.06.024.
[10] Wu X, Sun X, Guo Z, Tang J, Shen Y, James TD, Zhu W. In vivo and in situ tracking cancer chemotherapy by highly photostable NIR fluorescent theranostic prodrug. J Am Chem Soc 2014;136(9):3579–88. https://doi.org/10.1021/ja412380j.
[11] Zhiqian G, Sookil P, Yoon J, Shin I. Recent progress in the development of near-infrared fluorescent probes for bioimaging applications. Chem Soc Rev 2014;43:16–29. https://doi.org/10.1039/C3CS60271K.
[12] Strobl M, Walcher A, Mayr T, Klimant I, Borisov SM. Trace ammonia sensors based on fluorescent near-infrared-emitting aza-BODIPY dyes. Anal Chem 2017;89(5):2859–65. https://doi.org/10.1021/acs.analchem.6b04045.
[13] Bottaro E, Mosayyebi A, Carugo D, Nastruzzi C. Analysis of the diffusion process by pH indicator in microfluidic chips for liposome production. Micromachines 2017;8(7):209. https://doi.org/10.3390/mi8070209.
[14] Fan J, Sun W, Wang Z, Peng X, Li Y, Cao J. A fluorescent probe for site I binding and sensitive discrimination of HSA from BSA. Chem Commun 2014;50(67):9573–6. https://doi.org/10.1039/c4cc03778b.
[15] Deligeorgiev T, Vasilev A, Kaloyanova S, Vaquero JJ. Styryl dyes - synthesis and applications during the last 15 years. Color Technol 2010;126(2):55–80. https://doi.org/10.1111/j.1478-4408.2010.00235.x.
[16] Yang S, Liu Y, Feng G. Rapid and selective detection of fluoride in aqueous solution by a new hemicyanine-based colorimetric and fluorescent chemodosimeter. RSC Adv 2013;3:20171–8. https://doi.org/10.1039/C3RA42613K.
[17] Yu T, Yin G, Niu T, Yin P, Li H, Zhang Y, Yao S. A novel colorimetric and fluorescent probe for simultaneous detection of SO_3^{2-}/HSO_3^- and HSO_4^- by different emission channels and its bioimaging in living cells. Talanta 2018;176:1–7. https://doi.org/10.1016/j.talanta.2017.08.001.
[18] Zhang Y. Reversible fluorescent probe for selective detection and cell imaging of oxidative stress indicator bisulfite. Anal Chem 2016;88(8):4426–31. https://doi.org/10.1021/acs.analchem.6b00061.
[19] Fan J, Sun W, Wang Z, Peng X, Li Y, Cao J. A two-photon fluorescent probe with near-infrared emission for hydrogen sulfide imaging in biosystems. Chem Commun 2013;49:3890–2. https://doi.org/10.1039/C3CC41244J.
[20] Yu D, Huang F, Ding S, Feng G. Near-infrared fluorescent probe for detection of thiophenols in water samples and living cells. Anal Chem 2014;86(17):8835–41. https://doi.org/10.1021/ac502227p.
[21] Ma J, Fan J, Sun W, Wang Z, Peng X, Li Y, Cao J. Probing hydrazine with a near-infrared fluorescent chemodosimeter. Dyes Pigments 2017;138:39–46. https://doi.org/10.1016/j.dyepig.2016.11.026.
[22] Huang L, Yang Z, Zhou Z, Li Y. A dual colorimetric and near-infrared fluorescent turn-on probe for Hg^{2+} detection and its applications. Dyes Pigments 2019;163:118–25. https://doi.org/10.1016/j.dyepig.2018.11.047.
[23] Hongda L, Longyi J, Yuhe K, Bingzhu Y. A visual and "turn-on" fluorescent probe for rapid detection of cysteine over homocysteine and glutathione. Sens Actuators B 2014;196:546–54. https://doi.org/10.1016/j.snb.2014.02.052.
[24] Yang Y, Wang L, Xu M, Chen J, Qu Y. Triphenyl phosphate end-capped dicyanomethylene-4H-pyran as a near infrared fluorescent sensor for lysozyme in urine sample. Sens Actuators B Chem 2019;284:553–61. https://doi.org/10.1016/j.snb.2019.01.001.
[25] Wang X, Li P, Ding Q, Wu C, Zhang W, Tang B. Observation of acetylcholinesterase in stress-induced depression phenotypes by two-photon fluorescence imaging in the mouse brain. J Am Chem Soc 2019;141(5):2061–8. https://doi.org/10.1021/jacs.8b11414.
[26] Johnson I, Spence M. Molecular probes handbook: a guide to fluorescent probes and labeling Technologies. eleventh ed. Life Technologies; 2010.
[27] Martineau M, Somasundaram A, Grimm JB, Gruber TD, Choquet D, Taraska JW, Lavis LD, Perrais D. Semisynthetic fluorescent pH sensors for imaging exocytosis and endocytosis. Nat Commun 2017;8(1):1412. https://doi.org/10.1038/s41467-017-01752-5.
[28] Yahaya I, Chemchem M, Aydıner B, Seferoğlu N, Erva Tepe F, Açık L, Seferoğlu Z. Novel fluorescent coumarin-thiophene-derived schiff bases: synthesis, effects of substituents, photophysical properties, DFT calculations, and biological activities. J Photochem Photobiol A Chem 2019;368:296–306. https://doi.org/10.1016/j.jphotochem.2018.09.041.
[29] Olsen S, Baranov MS, Baleeva NS, Antonova MM, Johnson KA, Solntsev KM. pH-Sensitive fluorophores from locked GFP chromophores by a non-alternant analogue of the photochemical meta effect. Phys Chem Chem Phys 2016;18(38):26703–11. https://doi.org/10.1039/c6cp02423h.
[30] Langhals H, Rauscher M. NIR absorption of perylene dyes and fluorescence with large Stokes' shift by simple deprotonation. Z Naturforschung 2013;68b:683–6. https://doi.org/10.5560/ZNB.2013-3090.
[31] Li X, Gao X, Shi W, Ma H. Design strategies for water-soluble small molecular chromogenic and fluorogenic probes. Chem Rev 2013;114(1):590–659. https://doi.org/10.1021/cr300508p.
[32] Patsenker LD, Tatarets AL, Terpetschnig EA. Long-wavelength probes and labels based on cyanines and squaraines. In: Demchenko A, editor. Advanced fluorescence reporters in chemistry and biology I Springer series on fluorescence (methods and applications), vol. 8. Berlin, Heidelberg: Springer; 2010. p. 65. https://doi.org/10.1007/978-3-642-04702-2_3.
[33] Brouwer AM. Standards for photoluminescence quantum yield measurements in solution (IUPAC Technical Report). Pure Appl Chem 2011;83(12):2213–28. https://doi.org/10.1351/PAC-REP-10-09-31.
[34] Salgado LEV, Vargas-Hernández C. Spectrophotometric determination of the p*K*a, isosbestic point and equation of absorbance vs. pH for a universal pH indicator. Am

J Anal Chem 2014;5:1290–301. https://doi.org/10.4236/ajac.2014.517135.
[35] Bortolotto E, Rousseau R, Teodorescu B, Wielant A, Debauve G. Assessing similarity with parallel-line and parallel-curve models: implementing the USP development/validation approach to a relative potency assay. BioProcess Int 2015;13(6):26–37.
[36] Samuel TC, Robert CM. A facile one-pot conversion of aldehydes into nitriles. Synth Commun 2009;39(20):3601–6. https://doi.org/10.1080/00397910902788174.
[37] Bruna B, Casanova L, Mauro N, Michel MM, Fuentefria AM. Synthesis and biological evaluation of hydrazone derivatives as antifungal agents. Molecules 2015;20(5):9229–41. https://doi.org/10.3390/molecules20059229.
[38] Patil AM, Sayare AS, Chitlange S, Khadke AP, Pokharkar DV. Synthesis and biological evaluation of novel 2,4-thiazolidinedione derivatives as antibacterial agent. Asian J Chem 2012;24:5305–8.
[39] Bokan M, Bondar K, Marks V, Gellerman G, Patsenker L. Switchable phenolo-cyanine reporters containing reactive alkylcarboxylic groups for fluorescence-based targeted drug delivery monitoring. Dyes Pigments 2018;159:18–27. https://doi.org/10.1016/j.dyepig.2018.05.046.
[40] Kratz F, Beyer U, Roth T, Schütte MT, Unold A, Fiebig HH, Unger C. Albumin conjugates of the anticancer drug chlorambucil: synthesis, characterization, and in vitro efficacy. Arch Pharm Weinh 1998;331:47–53. https://doi.org/10.1002/(SICI)1521-4184(199802)331:2<47::AID-ARDP47>3.0.CO;2-R.
[41] He R, Finan B, Mayer JP, DiMarchi RD. Peptide conjugates with small molecules designed to enhance efficacy and safety. Molecules 2019;24:1855. https://doi.org/10.3390/molecules24101855.
[42] Gilad Y, Noy E, Senderowitz H, Albeck A, Firer MA, Gellerman G. Synthesis, biological studies and molecular dynamics of new anticancer RGD-based peptide conjugates for targeted drug delivery. Bioorg Med Chem 2016;24:294–303. https://doi.org/10.1016/j.bmc.2015.12.020.
[43] Tiwari AK, Sathyamurthy N. Structure and stability of salicylic acid-water complexes and the effect of molecular hydration on the spectral properties of salicylic acid. J Phys Chem A 2006;110(17):5960–4. https://doi.org/10.1021/jp060851e.
[44] Metsov S, Simov D, Stoyanovb S, Nikolov P. Photophysical characteristics of some 2-styrylindolium dyes. Dyes Pigments 1990;13:11–9. https://doi.org/10.1016/0143-7208(90)80009-E.
[45] Markova LI, Fedyunyayeva IA, YeA Povrozin, Semenova OM, Khabuseva SU, Terpetschnig EA, Patsenker LD. Water soluble indodicarbocyanine dyes based on 2,3-dimethyl-3-(4-sulfobutyl)-3H-indole-5-sulfonic acid. Dyes Pigments 2013;96:535–46. https://doi.org/10.1016/j.dyepig.2012.09.007.
[46] Markova LI, Terpetschnig EA, Patsenker LD. Comparison of a series of hydrophilic squaraine and cyanine dyes for use as biological labels. Dyes Pigments 2013;99:561–70. https://doi.org/10.1016/j.dyepig.2013.06.022.
[47] Kolosova OS, Shishkina SV, Marks V, Gellerman G, Hovor IV, Tatarets AL, Terpetschnig EA, Patsenker LD. Molecular structure and spectral properties of indolenine based norsquaraines versus squaraines. Dyes Pigments 2019;163:318–29https://doi.org/10.1016/j.dyepig.2018.12.007.
[48] Yang Y, Xia M, Zhao H, Zhang S, Zhang X. A cell-surface-specific ratiometric fluorescent probe for extracellular pH sensing with solid-state fluorophore. ACS Sens 2018;3:2278–85. https://doi.org/10.1021/acssensors.8b00514.
[49] Dunn GE, Kung F. Effect of intramolecular hydrogen bonding on ionization constants of substituted salicylic acids. Can J Chem 1966;44(11):1261–9. https://doi.org/10.1139/v66-188.